INTERFERENCE MITIGATION FOR BROADBAND L-DACS

M. Schnell, S. Brandes, S. Gligorevic, German Aerospace Center (DLR), 82234 Wessling, Germany
M. Walter, University of Ulm, 89069 Ulm, Germany
C. Rihacek, M. Sajatovic, B. Haindl, Frequentis AG, Innovationsstraße 1, 1100 Vienna, Austria

Abstract

One deployment option for the future broadband L-band Digital Aeronautical Communications System (L-DACS) is operating as an inlay system between two adjacent channels of the Distance Measuring Equipment (DME) system. Investigations for the Broadband Aeronautical Multi-carrier Communications (B-AMC) [1] system, one candidate for the broadband L-DACS, have shown that interference originating from DME systems operating in adjacent channels has a strong impact on the B-AMC system. To enable the utilization of spectral gaps between two adjacent DME channels, two efficient methods for mitigating the impact of interference are proposed and investigated for the B-AMC system, namely pulse blanking and erasure based decoding. Simulations show that the impact of DME interference onto the L-DACS can be reduced considerably by choosing an appropriate coding scheme to make the transmit signal robust against interference. The impact of interference is mitigated by means of the proposed methods, resulting in a performance close to the performance in the interference-free case.

Introduction

B-AMC is one of the technologies proposed for the future L-DACS. B-AMC is based on the "Broadband VHF Aeronautical Communications System based on MC-CDMA" (B-VHF) [2,3] developed in the B-VHF project co-funded by the European Commission between 2004 and 2006. During the joint Eurocontrol/FAA Future Communications Study (FCS) B-VHF was selected as one of the most promising technologies and put onto the technology short-list.

According to Eurocontrol and FAA roadmaps, new future air-ground radio systems should preferably be deployed in the L-band. In February 2007, Eurocontrol initiated the investigation of a B-VHF like system in the L-band which led to the development of the B-AMC system concept. A detailed assessment of B-AMC has been carried out within the FCS with very promising results. As final result of the FCS B-AMC together with P34 [4] have been chosen for the broadband L-DACS proposal. Apart from the broadband L-DACS, the FCS considers an L-DACS based on narrowband technologies, which is, however, out of the scope this paper.

Currently, the broadband L-DACS is being specified combining advantageous characteristics of B-AMC and P34 as well as of the IEEE 802.16e (WiMAX) [5] standard. Like B-AMC and P34, broadband L-DACS will employ orthogonal frequency-division multiplexing (OFDM) for modulation and apply Frequency-Division Duplex (FDD) to separate forward and reverse link (FL/RL) transmissions.

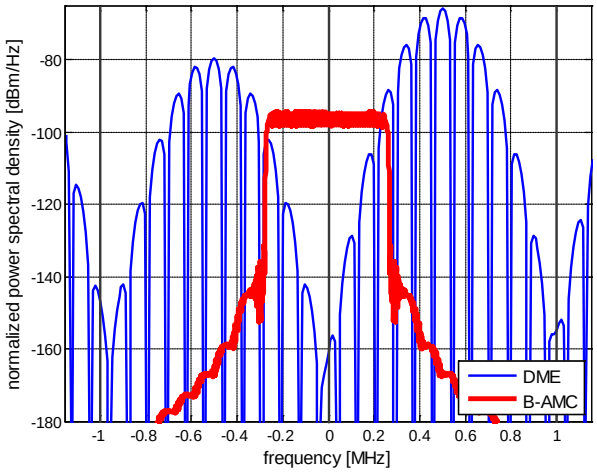

Figure 1: Inlay concept: B-AMC spectrum between two adjacent DME channels.

One promising deployment option for L-DACS is an inlay concept that allows the utilization of frequency gaps between two adjacent channels already assigned to other L-band systems such as the DME or the military tactical air navigation (TACAN) system. The inlay concept has already

been investigated for the B-AMC system. As illustrated in Figure 1, the B-AMC system uses a bandwidth of 500 kHz between two adjacent DME channels lying on the 1 MHz grid.

FL channels are envisaged to be located within the 979-1025 MHz sub-band and RL channels within the 1035-1085 MHz or alternatively within the 1095-1150 MHz sub-band. The inlay concept is especially attractive, since it enables the re-use of already assigned frequency spectrum without requiring changes of the legacy L-band systems. This challenging goal can only be achieved if the broadband L-DACS does not interfere with the existing legacy L-band systems and vice versa. Interference from the broadband L-DACS towards legacy L-band systems is avoided by applying out-of-band radiation reduction techniques already successfully developed for the B-VHF system. Co-site interference towards other airborne L-band receivers is alleviated by a low airborne transmitter utilization factor (e.g. low duty cycle). In addition, proper frequency planning assures that broadband L-DACS service volumes use frequency channels sufficiently far away from the DME frequencies used in nearby DME service volumes. L-band navigation systems such as DME and TACAN constitute the main source of interference for an inlay L-DACS system. Furthermore, military communications systems like the Joint Tactical Information Distribution System or the Multifunctional Information Distribution System (JTIDS/MIDS) also apply pulsed transmissions causing interference.

The topic of this paper is the mitigation of pulsed interference which has a significant impact on the performance of the broadband L-DACS receiver. Since the L-DACS is not yet specified, the investigations are based on the B-AMC system concept that has already been presented at last year's DASC [1]. However, in general, the proposed techniques are applicable to any OFDM system operated in the L-band and hence serve as input to the final specification of the broadband L-DACS.

In the next section of this paper, the B-AMC system model from [1] is briefly recapitulated. As a starting point for the investigations, the DME interference signal is characterized and an interference simulator for investigating its impact on the OFDM system is presented. In the following two sections, two different approaches for mitigating the impact of pulse interference are presented, namely pulse blanking and erasure decoding. Both methods are investigated analytically and by means of simple simulations. Finally, both methods are compared based on a common simulation scenario and conclusions are drawn.

System Model

A bandwidth of 500 kHz is considered to be available between two adjacent DME channels for each B-AMC channel (FL or RL). OFDM parameters are set taking into account the available bandwidth and L-band propagation conditions as described in [1].

Subcarrier spacing is chosen to be 10.416 kHz taking into account the coherence bandwidth of the transmission channel and the expected Doppler spread. Hence, 48 subcarriers are located within the available bandwidth and can be used for data transmission. At each edge of the B-AMC spectrum, eight guard subcarriers are inserted that are not used for data transmission. The resulting total 64 subcarriers are OFDM modulated by means of a 64-point Discrete Fourier Transform (DFT). The corresponding sampling frequency is 666.6 kHz and the equivalent sampling interval in the time domain is 1.5 μs.

According to the selected subcarrier spacing, the duration of one OFDM symbol equals 96 μs and is extended by a cyclic prefix to 120 μs. One half of the cyclic prefix serves as guard interval to avoid inter-symbol interference between successive OFDM symbols. The other half is used for transmitter windowing to reduce out-of-band radiation.

54 successive OFDM symbols are organized to one OFDM frame with a length of 6.48 ms. Subtracting special OFDM symbols for synchronization and channel estimation, 48 and 50 OFDM symbols remain for the transmission of useful data in the FL and RL, respectively. The main B-AMC system parameters are listed in Table 1.

Table 1: Basic B-AMC system parameters

Parameter	Value
Effective bandwidth	500 kHz (FL or RL)
Sub-carrier spacing	10.416 kHz
Used sub-carriers	N_{used} = 48
DFT length	N=64
Sampling interval/ Sampling frequency	1.5 μs f_s = 666.6 kHz
OFDM symbol duration	96 μs
Cyclic prefix	24 μs
Total OFDM symbol duration	T_O = 120 μs
OFDM symbols per frame	54
Data OFDM symbols per frame	48 (FL) 50 (RL)
OFDM frame duration	6.48 ms

Characterization and Modeling of L-Band Interference

The DME signal consists of pairs of Gaussian shaped pulses with a separation of Δt = 12 μs or 36 μs. One pulse pair in the base band is given by

$$p(t) = e^{-\alpha t^2/2} + e^{-\alpha (t-\Delta t)^2/2}.$$

The parameter $\alpha = 4.5 \cdot 10^{11}\ 1/s^2$ is set such that the time interval between the 50% amplitude point on the leading and trailing edge of the pulse envelope is 3.5 μs. For generating the interference signals in the channels directly adjacent to the B-AMC system, these pulse pairs are modulated to carriers with an offset relative to the center of the B-AMC channel, i.e. $f_{c,i}$ =± 500 kHz with *i=0,…,I-*1, denoting the index of the interferer. Interferers operating in DME channels at larger frequency offsets, i.e. at $f_{c,i} \geq \pm$ 1.5 MHz, are neglected as their impact is assumed to be reduced significantly by the intermediate frequency (IF) filter of the OFDM receiver. In the channels at $f_{c,i}$ =± 500 kHz offset to the B-AMC center frequency, the interference signals of multiple DME stations superimpose. Each of the I contributing DME stations is typically received with different a power level P_i and different pulse rate. According to the pulse rate of the ith station, L_i pulse pairs are generated in the observed time interval. The starting times $t_{i,l}$ of the pulse pairs are modeled as a Poisson process. The phases $\varphi_{i,l}$ are equally distributed in the interval $[0, 2\pi]$. The resulting interference signal composed of contributions from I active DME stations is given by

$$i(t) = \sum_{i=0}^{I-1} \sum_{l=0}^{L_i-1} \sqrt{P_i}\, p(t - t_{i,l}) e^{j 2\pi f_{c,i} t + \varphi_{i,l}}.$$

At the B-AMC receiver, the received signal is composed of the desired OFDM signal and the interference signal. In order to model the impact of interference onto the B-AMC signal as realistically as possible, the interference signal is processed in the same way as the OFDM signal would be processed at the receiver. Therefore, the interference signal is first filtered by the IF band-pass filter, which is assumed to have the same characteristics as commonly used DME equipment. Its filter characteristic is derived from filter characteristics of commercially available DME equipment and adjusted to the receiver bandwidth of the OFDM system. When sampling the received signal with sampling frequency f_s, the Nyquist sampling theorem is violated for the interference signal, since the bandwidth of the B-AMC system, the sampling frequency f_s is tailored to, is smaller than the bandwidth of the interference signal. This results in periodic repetitions of the interference spectrum with periodicity f_s that partly coincide with the OFDM bandwidth, hence causing additional interference. To overcome this problem over-sampling is introduced. In the considered OFDM system with f_s = 666.6 kHz, four-times over-sampling is used to increase the sampling frequency to 2.66 MHz. In addition, an anti-aliasing filter is applied to diminish influences of DME interference signals in channels at larger offsets. For that purpose, a standard raised-cosine filter with roll-off factor 0.22 is used, as applied in the Universal Mobile Tele-communications System (UMTS). Its bandwidth is adjusted to the bandwidth of the B-AMC system. The impulse responses of both the IF and the anti-aliasing filter are combined to the filter characteristic *f(t)* and the resulting filtered interference signal writes

$$i^{(f)}(t) = f(t) * i(t),$$

where '*' denotes convolution.

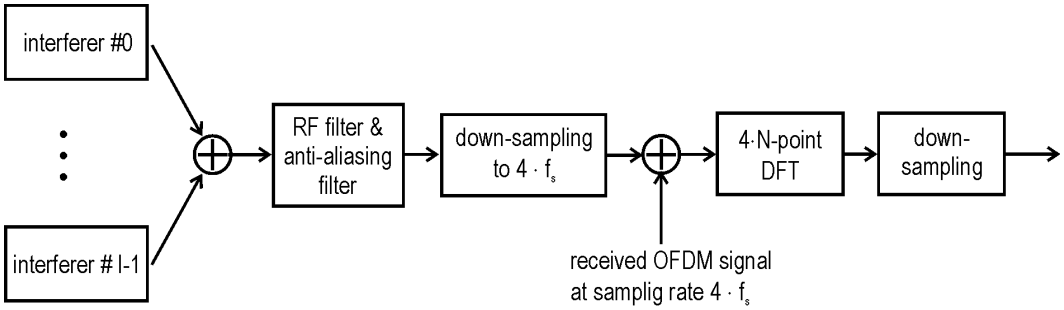

Figure 2: Block diagram of interference simulator.

When modeling the desired OFDM signal, the filters can be neglected as in the ideal case, they do not affect the OFDM signal lying in the pass-band of the combined filters. However, over-sampling has to be taken into account by over-sampling the B-AMC signal as well prior to adding interference to the OFDM signal. To transform the resulting signal to the frequency domain, the DFT length has to be increased accordingly. Afterwards, the resulting signal composed of interference and desired signal is down-sampled to the target OFDM sampling rate.

The resulting block diagram of a simulator for DME interference is shown in Figure 2. Note, in the interference simulator, the *I* interference signals are generated quasi-continuously with 16-times over-sampling and are down-sampled to sampling rate 4 f_s after filtering. Effects of analog-to-digital conversion are not taken into account.

The impact of DME interference in the FL is simulated for an interference scenario representing severe interference conditions. As the B-AMC FL is intended to be operated in the sub-band 979-1025 MHz, except for the "own" airborne DME interrogator, which is neglected here, only DME ground stations cause interference at the B-AMC airborne receiver. The real DME channel allocation is modeled with the NAVSIM[1] tool [6] for the area around Paris as this is the area with the highest density of DME ground stations in Europe. The victim B-AMC receiver is positioned at an en-route flight level at 45,000 feet altitude in the center of this area. The peak interference power originating from each ground DME/TACAN station is determined via simple link budget calculations, taking into account free space loss and elevation angle dependent antenna gains that are derived from directive antennas of standard DME equipment. In this particular example, severe interference conditions are observed when the B-AMC system is operated at 995.5 MHz. In this scenario, only interferers in the channels at ± 0.5 MHz offset to the B-AMC center frequency are considered. Interference from DME stations in channels at larger offsets are supposed not to impair the B-AMC system significantly due to their larger separation in frequency and their spatial distance. The considered interference scenario is listed in Table 2.

Table 2: Interference Scenario

Station	Frequency [MHz]	Interference power at victim RX input	Pulse rate (ppps)
TACAN	995	-67.9 dBm	3600
B-AMC	995.5		
TACAN	996	-74.0 dBm	3600
TACAN	996	-90.3 dBm	3600

As can be seen from Figure 1, when DME interference occurs, a significant fraction of the OFDM subcarriers is affected. One TACAN station may transmit up to 3600 pulse pairs per second (ppps). In the considered interference scenario, three TACAN stations occur in both adjacent channels. As the pulses of the three stations are statistically independent, their pulse rates can be represented by one random process producing a total pulse rate as high as 10800 ppps. Modeling the starting times of the pulse pairs as a Poisson process, the probability that an OFDM symbol is hit by DME interference is given by the

[1] The Air Traffic / ATC & CNS simulation tool "NAVSIM" has been developed by "Mobile Communications R&D GmbH, Salzburg" in close co-operation with University of Salzburg.

complementary probability of the event that no interference occurs within an OFDM symbol, i.e.

$$P_{hit} = 1 - e^{-\lambda(T_O + 3.5\mu s)}$$

with T_O denoting the duration of an OFDM symbol which is 96 µs for the considered B-AMC system. Note, the cyclic prefix is neglected in this consideration, since it is discarded at the OFDM receiver anyway and pulses in the cyclic prefix do not impair the data bearing part of the OFDM symbol. However, the observed interval has to be extended by the duration of one pulse to take into account pulses at the end of an OFDM symbol. The intensity λ of the Poisson process is determined by the number of pulses which is $2 \cdot 10800$ pulses per second in the regarded example. With the given parameters, the probability that an OFDM symbol is hit by DME interference is 88%. The probability that one OFDM symbol is hit by two pulses is as high as 25%.

Taking into account the sampling rate of the OFDM system that is 1.5 µs or 0.375 µs without or with four times over-sampling, about three or 12 samples of the desired signal are affected when a DME pulse occurs, respectively. Due to the high duty cycle and high power, DME interference has a severe impact on the performance of the B-AMC system and hence has to be mitigated.

Interference Mitigation by Pulse Blanking or Clipping

As the power level of the DME pulses usually exceeds the received signal level of the desired OFDM signal, DME pulses can be detected in the time domain received signal. A straightforward and simple approach for mitigating the impact of DME interference is pulse blanking. As illustrated in Figure 3, the samples affected by interference are cut out by setting them to '0'. This approach is also applied for mitigating DME interference in satellite navigation systems in the E5 and L5 band at 1176.45 MHz and 1207.14 MHz [7]. Although very simple, pulse blanking suffers from the drawback that the desired OFDM signal is blanked as well, when a DME pulse occurs. The resulting loss in signal-to-noise ratio (SNR) and bit error rate (BER) performance can be kept at a minimum by properly choosing the threshold for blanking as a trade-off between interference reduction and impairment of the desired OFDM signal.

Alternatively or even additionally, clipping [8] can be applied which is also illustrated in Figure 3. In that case, samples affected by interference are set to the threshold rather than erasing them as for pulse blanking. However, clipping is not further addressed in this paper.

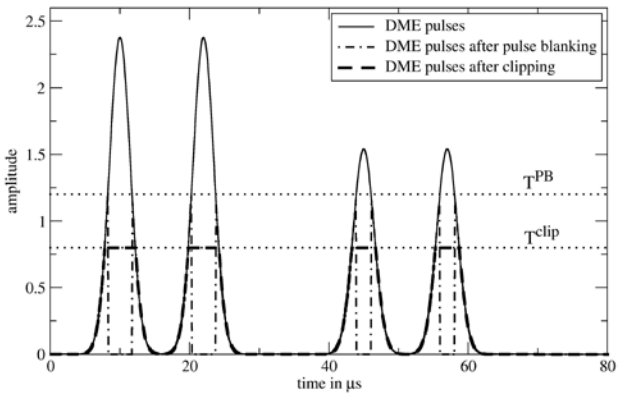

Figure 3: Principle of pulse blanking and clipping.

Before either of both approaches can be applied, DME pulses need to be detected in the received OFDM signal. A non-constant signal level with peaks is an inherent property of the OFDM signal resulting in a high peak-to-average power ratio (PAPR) even without interference. With a mere threshold decision, peaks in the OFDM signal would falsely be detected as DME pulses. Blanking or clipping these falsely detected pulses affects the desired B-AMC signal and degrades performance without reducing the impact of interference.

This problem can be easily overcome by taking into account the number of subsequent samples exceeding the threshold. Investigations have shown that, in the four-times over-sampled received signal, 1 to 8 subsequent samples with amplitude above the threshold are mostly caused by a peak in the OFDM signal. More than 8 samples exceeding the threshold suggest a DME pulse. Consequently, DME pulses are detected by identifying the samples in the received signal that exceed the threshold in a first step. Second, single or pairs of two detected samples are sorted out, as they are more likely peaks in the OFDM signal rather than fractions of DME pulses.

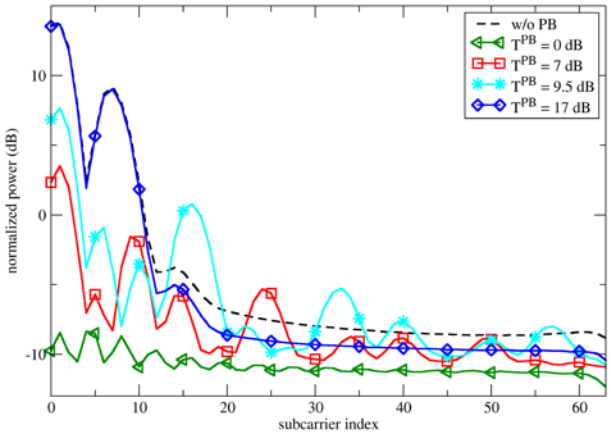

Figure 4: Spectrum of DME signal after pulse blanking with different thresholds.

The influence of the choice of the threshold for pulse blanking is illustrated in Figure 4 for a DME interferer at -0.5 MHz offset to the OFDM system. In the example, the power of the interferer is -75 dBm, which is normalized such as to give a signal-to-interference power ratio (SINR) of -3.8 dB with the power of the desired OFDM signal being normalized to 0 dB and SNR set to 10 dB.

When the threshold is set to the same level as the average power of the desired OFDM signal, i.e. T^{PB} = 0 dB, pulse blanking reduces the interference power to the noise level on nearly all subcarriers. With increasing threshold, interference power increases, but, on the average, always remains below the interference power without pulse blanking. However, on some subcarriers interference power increases compared to the case without pulse blanking. This is due to the fact, that fractions of DME pulses remain after pulse blanking and cause sharp phase transitions in the time domain signal that result in spectral peaks. When the threshold is set nearly to the maximum power of the interference signal, T^{PB} = 17 dB, interference power is only slightly reduced. With respect to interference power reduction the threshold should be set as low as possible. However, this goes in with a significant impairment of the desired OFDM signal, as a significant fraction of the OFDM signal is blanked as well. Hence, the threshold has to be optimized as a trade-off between interference power reduction and impact on the desired OFDM signal.

In [8, 9], the optimal threshold for pulse blanking and clipping has been derived analytically for impulsive noise. Since the structure of DME interference is far more complex, this approach cannot be easily extended to DME interference. Hence, the optimal threshold for pulse blanking is determined by means of systematic simulations with one DME interferer with different pulse rate and power in the channel at 0.5 MHz offset to the B-AMC system.

In the simulations, B-AMC parameters are assumed. All OFDM symbols within one frame are used for transmitting QPSK modulated data coded with a rate ½ convolutional code. The variance of the AWGN channel is set such as to obtain SNR = 5 dB. The average received power of the OFDM signal is normalized to 1 (0 dB). The power of the interference signal is adapted accordingly such as to give SINR values of -4.1 dB, -7.0 dB, and -8.5 dB when an interferer with -70 dBm power and pulse rate 3600 ppps, 7200 ppps, and 10800 ppps is considered, respectively. For an interferer with -75 dBm and 7200 ppps or 10800 ppps, SINR equals -2.5 dB or -3.8 dB, respectively. In the simulations, perfect detection of DME pulses has been assumed in order to be able to neglect impairments of inaccuracies in pulse detection.

In Figure 5, the BER after pulse blanking versus threshold is given for different interferers as listed above. The threshold is normalized to the average power of the received signal which is 1, respectively. The BER without pulse blanking is given as reference for each interferer. In general, high BER is observed when the threshold is set too low. In that case, interference is reduced considerably, but at the same time the desired OFDM signal is affected as a significant fraction of the OFDM signal is blanked. For high thresholds >17 dB for interferers with -70 dBm power and >12 dB for interferers with -75 dBm power, the impact of interference is hardly reduced resulting in a BER close to the BER without pulse blanking. As expected, this point is reached 5 dB earlier for interferers with -75 dBm power than for interferers with -70 dBm power. Nevertheless, even for high thresholds, BER is slightly better than without pulse blanking. This can be explained as follows. At the beginning and at the end of an OFDM symbol, the interference signal may exhibit very high amplitudes occurring when only a fraction of a DME pulse coincides with the OFDM symbol.

These samples are removed by pulse blanking with very high threshold, hence slightly improving BER performance.

Before the performance of the case without pulse blanking is reached, a maximum occurs in the curves for the interferers with -70 dBm power. In this threshold region, performance is dominated by interference and already lies close to the case without pulse blanking. However, a few samples of the interference signal are still blanked which mainly causes additional bit errors and increases the total BER.

For the interferers with -75 dBm power, the curves exhibit a minimum before the performance of the case without pulse blanking is reached. For threshold <12 dB, performance is already dominated by the reduction of interference power rather than by the number of blanked samples in the desired OFDM signal. However, this minimum is not considered to be a feasible threshold, as the actual interference conditions, e.g. according to the scenario in Table 2, are more likely to be determined by interferers with higher power.

For interferers with -70 dBm peak power, the lowest BER is achieved for a threshold 6 dB above the average power of the desired B-AMC signal, independent of the pulse rate. With that threshold, for an interferer with 10800 ppps, 79 out of 256 samples of an OFDM symbol are blanked on the average. First, this reduces the power of the OFDM signal and results in an SNR loss as high as 1.6 dB for the considered example. Second, BER increases considerably due to lacking parts in the OFDM signal. Parts of these losses are counterbalanced by the reduction of interference power induced by blanking. The average interference power is reduced from -102.4 dBm to -120.6 dBm. Note, these values differ from the nominal peak power of the interferer as an average interference power is calculated within the B-AMC bandwidth only and the DME duty cycle is taken into account as well.

For interferers with -75 dBm peak power, the optimal threshold is 8 dB above the average power of the OFDM signal for both the interferer with 7200 ppps and 10800 ppps. For the interferer with 10800 ppps, 44 out of 256 samples are blanked per OFDM symbol on the average. The average interference power is reduced from -107.4 dBm to -114.7 dBm which is higher than for the interferer with -70 dBm. Setting the threshold to 6 dB as for the interferer with -70 dBm power would result in an average interference power as low as -120.6 dBm, but the total BER would be slightly higher as more samples are blanked.

As according to the interference scenario from Table 2, interferers with high power and a total pulse rate of 10800 ppps are expected, the threshold for pulse blanking is set to 6 dB.

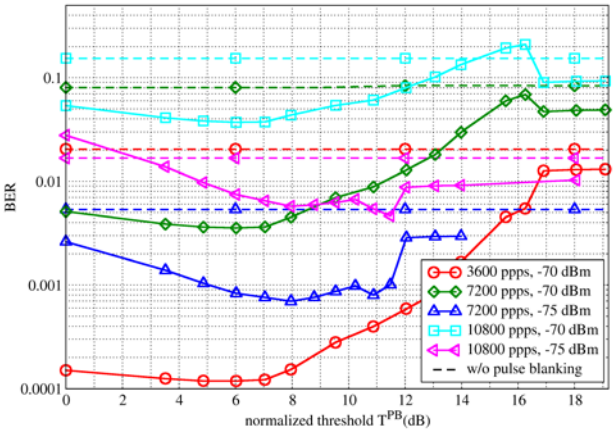

Figure 5: Optimal threshold for blanking one interferer at -0.5 MHz offset with different pulse rate and power, SNR = 5 dB.

To validate the choice of the threshold, the BER of pulse blanking in the interference scenario from Table 2 is shown in Figure 6. The best results are achieved for T^{PB} = 6 dB. With this choice of the threshold, the impact of interference is reduced by 4.3 dB at BER = 10^{-3}. The remaining gap between the performance after pulse blanking and the interference free case is explained by the impact of pulse blanking on the desired OFDM signal. Therefore, the performance of the OFDM signal with blanks but without interference is given as well. At BER = 10^{-3}, SNR loss is as high as 2.1 dB which is partly explained by the reduced the signal power and the additional bit errors both induced by erasing parts of the received signal.

In addition, different approaches for pulse detection are compared. With a simple threshold decision, performance of pulse blanking is considerably worse. With the improved pulse detection as proposed above, performance is considerably better.

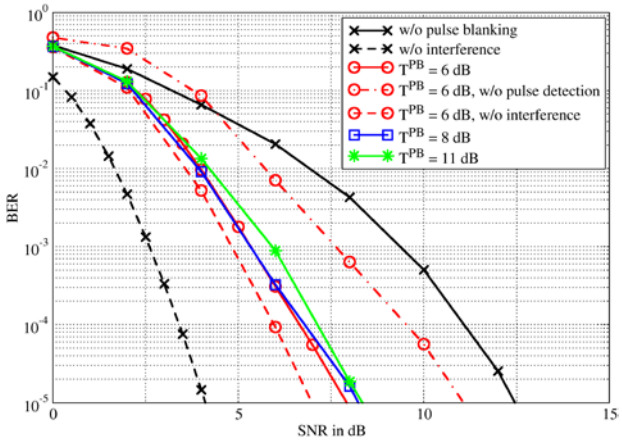

Figure 6: BER performance with pulse blanking.

Interference Mitigation by Erasure Decoding

Concatenated coding systems using a convolutional code (CC) for the inner code, and a Reed Solomon (RS) code as outer code are often applied for forward error correction when transmitting information over unreliable channels [10]. The inner convolutional code is used to correct random errors and the outer Reed Solomon code is able to correct error bursts produced by the Viterbi decoder. The same concatenation scheme and erasure based decoding is proposed for B-AMC.

A convolutional code provides sufficient random error correction on the inner subcarriers that are hardly affected by DME interference. As can be seen from Figure 1, the outer subcarriers are severely impaired by DME interference. Coding in time direction is thus orthogonal to the interference of one DME interferer and should avoid error bursts caused by DME interference. However, system performance still suffers if a large number of symbols is affected by DME interference preventing the convolutional decoder to return to the correct path in the trellis. Therefore, assuming 88% of the symbols affected by the DME interference according to the interference scenario from Table 2, frequency direction coding may be preferable for sufficiently high SNR values. Still, in both cases the DME interference pattern causes long error bursts at the convolutional decoder output limiting the performance of the outer RS decoder.

The effects of DME interference are reduced by randomly interleaving all bits within an OFDM frame. A random interleaver after the convolutional encoder spreads the erroneous symbols over one frame and thus, significantly improves the CC performance for sufficiently high SNR values.

If data of one frame is divided in more than one RS code word, an additional block interleaver is advantageous. A block interleaver between RS and CC encoder spreads the symbol errors of the CC decoder over all RS code words, i.e. reduces the number of erroneous symbols in a single code word, thus enabling better RS decoder performance.

The performance of the CC decoder with and without random interleaver and of the code concatenation is illustrated in Figure 7 for an AWGN channel with interference conditions according to Table 2. Transmitted frames contain only QPSK modulated data symbols, coded with the outer RS(2^8,162,146) code capable of correcting 8 bytes, and the rate ½ and constraint length 7 convolutional code with generator polynomials (171,133).

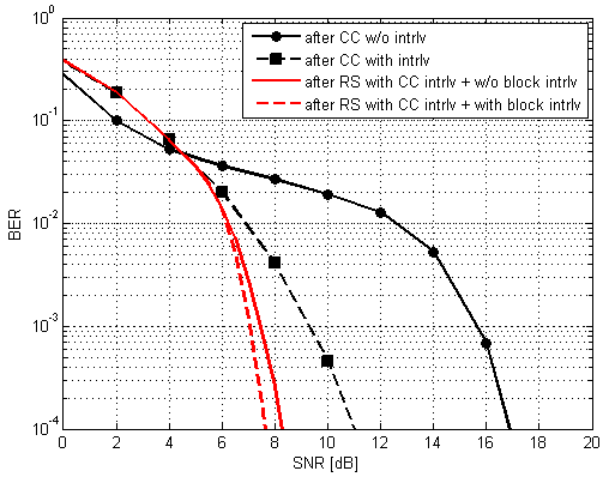

Figure 7: BER performance of convolutional code and concatenated code in interference scenario defined in Table 2.

Erasure decoding is one way to improve the code performance, for both convolutional and block code. Especially in the considered DME interference conditions, erasure decoding provides a

significant gain and enables reliable communication.

The received sequence can be converted into reliability information for each code bit and preceded to the Viterbi decoder. The reliability of a binary random variable x_i can be evaluated in terms of log-likelihood values by

$$L(x_i) = \ln\left(\frac{\sum_{x \in X} P(x_i = 1 \mid y)}{\sum_{x \in X} P(x_i = 0 \mid y)}\right) \text{ with } X = \{x_i, i = 1,..M \mid x_i = 0,1\}$$

where M represents the size of the modulation alphabet. Symbols affected by DME interference will falsely turn out to be most reliable, while the actual SINR on these symbols degrades. One way of defining erasures is based on the estimation of DME interference and the subsequent identification of subcarriers that are affected by DME interference. In the B-AMC system, interference detection is provided on the unused subcarriers at each side of the spectrum. On these subcarriers, the interference power level can be measured and the spectrum of the interference signal on all subcarriers can be reconstructed. Thereby, the spectral shape of the DME signal is assumed either to decay linearly or the actual DME spectrum is approximated based on known spectral characteristics of Gaussian shaped-pulses. In Figure 8, both estimations of the DME interference are illustrated. Reliability information of symbols for which the estimated SINR value is below a certain threshold is then set to zero. An example of estimated SINR over an OFDM symbol affected by DME interference and the corresponding erasure setting is presented in Figure 9. In the considered example the threshold is set to 0 dB.

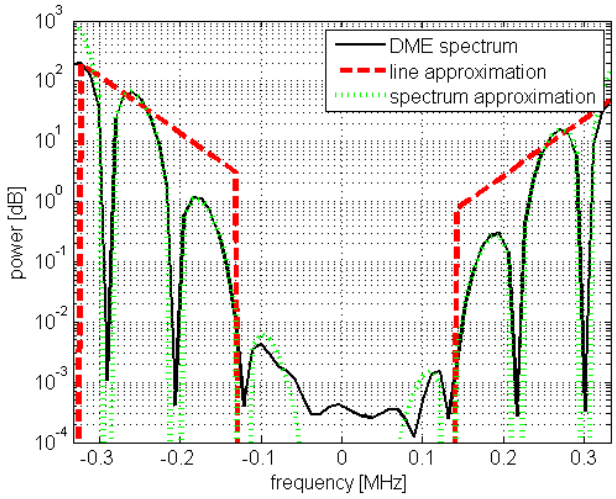

Figure 8: Interference estimation.

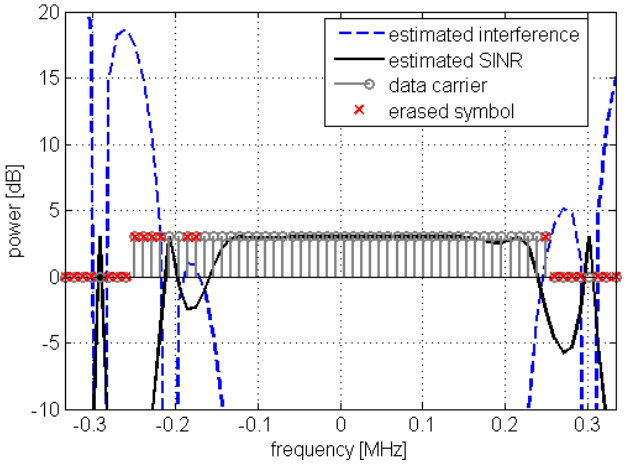

Figure 9: SINR estimation and erasure settings.

The performance of the proposed coding scheme with erasure settings at the convolutional decoder input is simulated in Figure 10. Only with the convolutional code a gain of approximately 4 dB is achieved at BER=10^{-2}. The performance loss after the RS decoder in comparison with AWGN channel is reduced to 1.1 dB. A small improvement with spectrum approximation for interference estimation in comparison with linear interference approximation can also be observed.

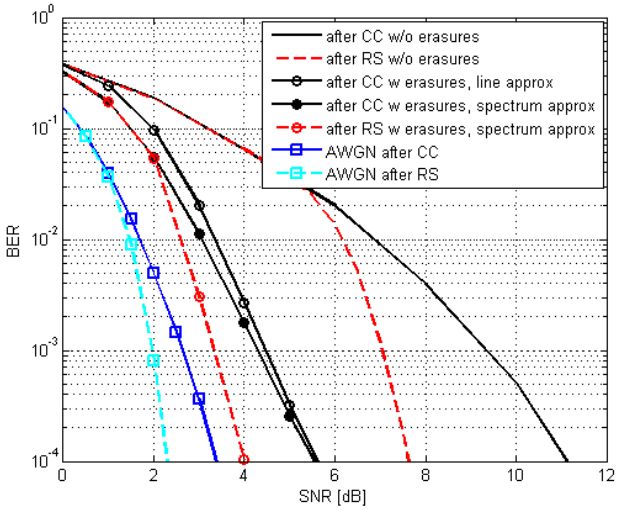

Figure 10: BER simulations with and without erasure based convolutional decoding.

By using the reliability information provided by the Soft Output Viterbi Algorithm (SOVA) [11], erasures can be set at the RS decoder input [12]. One simple way for defining erasures is given by setting the symbols containing the least reliable bits to erasures. If the erasures are set at the correct locations, more errors can be corrected by the decoding algorithm. However, declaring erasures at the RS decoder input also increases the probability for a decoding error [13].

The frequency domain error and erasure decoding [14] is applied in the simulations and results are presented in Figure 11. For low SNR values, the number of errors after the SOVA decoder is still above the error and erasures correction capability of the used RS code. At higher SNR values the reliability information provided by the SOVA will be more accurate and the number of errors after the CC decoder reaches a level, where they can be decoded correctly by benefitting from the erasures set at the decoder input.

The improvement in the BER that can be achieved with RS erasure decoding is however much less than the gain that results through CC erasure decoding. Figure 11 presents the results obtained with both a random and a block interleaver and applying erasures for the convolutional decoder. A small gain with additional RS erasure decoding is achieved for an SNR value above 3.5 dB.

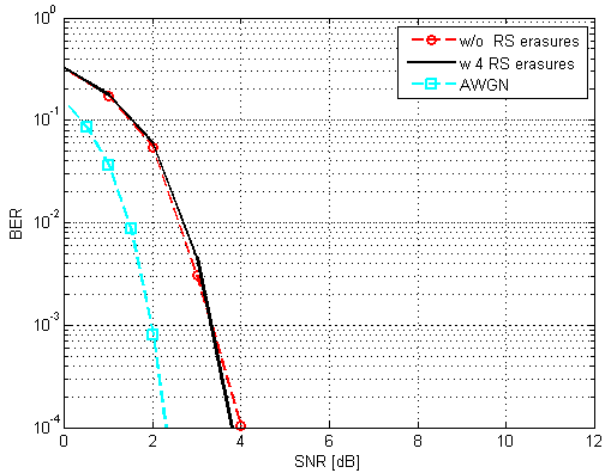

Figure 11: BER simulations with and without erasure based RS decoding.

Simulation Results

For comparing the performance of both approaches for interference mitigation, the two proposed methods are simulated in the same scenario.

QPSK modulated data are encoded with the outer RS(2^8,162,146) code and the inner convolutional code with generator polynomials (171,133), rate ½ and constraint length 7. As perfect synchronization and channel estimation are assumed, all OFDM symbols within one OFDM frame can be used for data transmission. At the output of the CC encoder, all bits are interleaved randomly; a block interleaver is not considered.

The transmission channel is modeled as an AWGN channel. Similar performance is expected when simulating the conditions at an en-route flight level that are mainly characterized by a strong line-of sight path. Interference is modeled according to the scenario defined in Table 2.

In contrast to the simulation results presented above, in this section frame error rate (FER) is considered instead of BER. Since higher layer protocols require a certain minimum FER performance to be able to operate properly, FER inherently determines the working point of the system. The target FER for the B-AMC system has been determined to be 10^{-2} [1].

Simulation results are given in Figure 12. The FER after CC and RS decoding without interference is given as reference. Without interference mitigation and without random interleaving, the impact of interference degrades performance by about 12 dB. As expected random interleaving improves performance considerably by about 5 dB. Applying pulse blanking and setting the threshold 6 dB above the average power of the OFDM signal, which has shown to be the optimal threshold, the SNR required to achieve FER = 10^{-2} reduces to 4.8 dB. Even better results are obtained with setting erasures at the input of the convolutional decoder. Erasures are determined based on an approximation of the DME spectrum and the threshold for the estimated SINR is set to 0 dB. With these parameters, the SNR to achieve the target FER is as low as 3.9 dB.

With simple link budget considerations this translates to a minimum required average received OFDM signal power of -104.1 dBm. Assuming a target cell size of 120 nm for an en-route cell, transmit power has to be at least 33.1 dBm, which is a reasonable value, even with respect to interference caused at DME and other L-band systems.

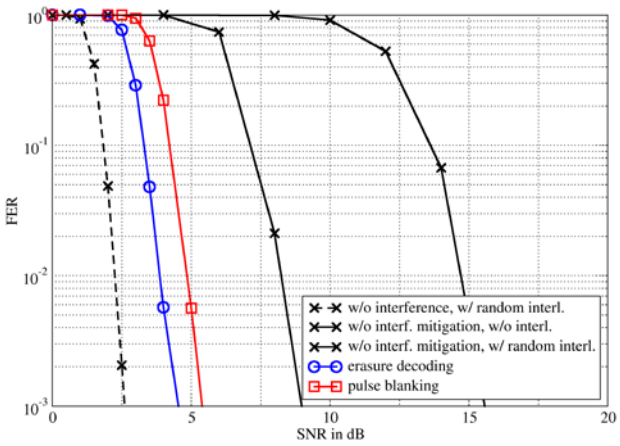

Figure 12: FER performance with different techniques for interference mitigation.

Conclusions and Outlook

Deploying the broadband L-DACS as an inlay system between two adjacent channels used by the DME/TACAN system is a promising approach for using the available L-band spectrum efficiently without requiring dedicated channel assignments for L-DACS. However, the L-DACS receiver is exposed to severe interference from legacy L-band systems. In this paper, pulse blanking and erasure decoding have been proposed for mitigating the impact of L-band interference onto the L-DACS. Simulations in a realistic interference scenario with the parameters of the B-AMC system have shown that both proposed methods are capable of reducing the impact of interference considerably, with erasure decoding performing better than pulse blanking.

Further investigations considering worse DME interference conditions as well as additional sources of interference will be required for L-DACS. The potentially resulting more stringent requirements for interference reduction can be meet by properly combining both approaches.

References

[1] C.-H. Rokitansky, M. Ehammer, Th. Gräupl, M. Schnell, S. Brandes, S. Gligorevic, C. Rihacek, and M. Sajatovic, “B-AMC A system for future Broadband Aeronautical Multi-Carrier communications in the L-Band,” Proc. *26th IEEE/AIAA Digital Avionics Systems Conference (DASC 2007)*, Dallas, Texas, USA, pp. 4.D.2-1 - 4.D.2-13

[2] I. Cosovic, S. Brandes, M. Schnell, B. Haindl, “Physical Layer Design for a Broadband Overlay System in the VHF-Band”, *24th IEEE/AIAA Digital Avionics Systems Conference (DASC 2005)*, Washington, D.C, USA, Oct./Nov. 2005.

[3] S. Brandes, M. Schnell, C.-H. Rokitansky, et al., “B-VHF – System Simulation Results and Final Assessment”, Proc. *25th IEEE/AIAA Digital Avionics Systems Conference (DASC 2006)*, Portland, OR, USA, Oct. 2006.

[4] TIA-902 (P34) Standard: http://www.tiaonline.org/standards/

[5] IEEE 802.16e (WiMAX) Standard: http://standards.ieee.org/getieee802/

[6] EUROCONTROL, "VDL Mode 2 Capacity Analysis through Simulations, WP3.B – NAVSIM Overview and Validation Results", Edition: 1.2, Oct. 2005.

[7] G. X. Gao, “DME/TACAN Interference and its Mitigation in L5/E5 Bands,” in *ION Institute of Navigation Global Navigation Satellite Systems Conference*, 2007.

[8] S. V. Zhidkov, “Analysis and Comparison of Several Simple Impulsive Noise Mitigation Schemes for OFDM Receivers,” *IEEE Transactions on Communications*, vol. 56, no. 1, pp. 5–9, January 2008.

[9] S. V. Zhidkov, “Performance Analysis and Optimization of OFDM Receiver With Blanking Nonlinearity in Impulsive Noise Environment,” *IEEE Transactions on Vehicular Technology*, vol. 55, no. 1, pp. 234–242, January 2006.

[10] W.W. Wu, D. Haccoun, R. Peile, Y. Hirata “Coding for Satellite Communication,” *IEEE Journal on Selected Areas in Comm.*, vol. SAC-5, no. 4, pp. 724-748, May 1987.

[11] J. Hagenauer, P. Hoeher, “A Viterbi algorithm with soft-decision outputs and applications,“ *Proc. IEEE Global Telecommunication Conference*, Dallas, Texas, Nov. 1989, pp. 1680-1686.

[12] S.C. Kwatra, P.M. Marriott, “Investigation of the Use of Erasures in a Concatenated Coding Scheme,“ *Technical Report submitted to NASA Lewis Research Center*, Cleveland, Ohio, June 1997.

[13] E.R. Berlekamp, “Readable Erasures Improve the Performance of Reed-Solomon Codes,” *IEEE Transactions on Information Theory*, Vol. IT-24, No. 5, September 1978.

[14] R.E. Blahut, *Algebraic codes for data transmission*, first ed., Cambrigde University Press, Cambrigde, 2003.

Email Addresses

Michael.Schnell@dlr.de

Sinja.Brandes@dlr.de

Snjezana.Gligorevic@dlr.de

M.Walter@dlr.de

Christoph.RIHACEK@frequentis.com

Miodrag.SAJATOVIC@frequentis.com

Bernhard.HAINDL@frequentis.com

27th Digital Avionics Systems Conference
October 26-30, 2008